

Relativistic calculations on the transition electric dipole moments and radiative lifetimes of the spin-forbidden transitions in the antimony hydride molecule

Yong Liu(刘勇), Lu-Lu Li(李露露), Li-Dan Xiao(肖利丹), and Bing Yan(闫冰)

Citation: Chin. Phys. B, 2022, 31 (**8**): 083101. DOI: 10.1088/1674-1056/ac6ee1
Journal homepage: http://cpb.iphy.ac.cn; http://iopscience.iop.org/cpb

What follows is a list of articles you may be interested in

Theoretical study on the transition properties of AlF

Yun-Guang Zhang(张云光), Ling-Ling Ji(吉玲玲), Ru Cai(蔡茹),Cong-Ying Zhang(张聪颖), and Jian-Gang Xu(徐建刚)

Chin. Phys. B, 2022, 31 (**5**): 053101. DOI: 10.1088/1674-1056/ac3648

Configuration interaction study on low-lying states of AlCl molecule

Xiao-Ying Ren(任笑影), Zhi-Yu Xiao(肖志宇), Yong Liu(刘勇), and Bing Yan(闫冰)

Chin. Phys. B, 2021, 30 (**5**): 053101. DOI: 10.1088/1674-1056/abd46a

Effects of electron correlation and the Breit interaction on one- and two-electron one-photon transitions in double K hole states of He-like ions ($10 \le Z \le 47$)

Xiaobin Ding(丁晓彬), Cunqiang Wu(吴存强), Mingxin Cao(曹铭欣), Denghong Zhang(张登红), Mingwu Zhang(张明武), Yingli Xue(薛迎利), Deyang Yu(于得洋), Chenzhong Dong(董晨钟)

Chin. Phys. B, 2020, 29 (**3**): 033101. DOI: 10.1088/1674-1056/ab6c51

Low-lying electronic states of aluminum monoiodide

Xiang Yuan(袁翔), Shuang Yin(阴爽), Yi Lian(连艺), Pei-Yuan Yan(颜培源), Hai-Feng Xu(徐海峰), Bing Yan(闫冰)

Chin. Phys. B, 2019, 28 (**4**): 043101. DOI: 10.1088/1674-1056/28/4/043101

Forbidden transition properties of fine-structure $2p^3\,{}^4S_{3/2}$-$2p^3\,{}^2D_{3/2,5/2}$ for nitrogen-like ions

Xiao-Kang He(何晓康), Jian-Peng Liu(刘建鹏), Xiang Zhang(张祥), Yong Shen(沈咏), Hong-Xin Zou(邹宏新)

Chin. Phys. B, 2018, 27 (**8**): 083102. DOI: 10.1088/1674-1056/27/8/083102

DATA PAPER

Relativistic calculations on the transition electric dipole moments and radiative lifetimes of the spin-forbidden transitions in the antimony hydride molecule

Yong Liu(刘勇), Lu-Lu Li(李露露), Li-Dan Xiao(肖利丹), and Bing Yan(闫冰)†

Institute of Atomic and Molecular Physics, Jilin University, Changchun 130012, *China*

(Received 6 March 2022; revised manuscript received 6 May 2022; accepted manuscript online 12 May 2022)

Calculations on the spectroscopic constants and transition properties of the first three states ($a^1\Delta$, $b^1\Sigma^+$, and $X^3\Sigma^-$) of the SbH molecule were performed under the relativistic framework using the exact two-component Hamiltonian (X2C). The potential energy curves in the Franck–Condon region were computed and compared with the previous values. Furthermore, the transition dipole moments for the weak spin-forbidden transitions ($b0^+$–$X_1 0^+$, $b0^+$–$X_2 1$, $X_1 0^+$–$X_2 1$, and $X_2 1$–a2) were reported. The spontaneous radiative lifetime of the $b^1\Sigma^+$ ($v' = 0$) state was calculated as 163.5 ± 7.5 μs, which is in reasonable agreement with the latest experimental value of 173 ± 3 μs. The spontaneous radiative lifetimes of the $X_2 1$ ($v' = 0$) state and the a2 ($v' = 0$) state were calculated to be 48.6 s and ∼ 8 ms, respectively. Our study is expected to be a benchmark transition property computation for comparison with other theoretical and experimental results. The datasets presented in this paper, including the transition dipole moments, are openly available at https://dx.doi.org/10.11922/sciencedb.j00113.00018.

Keywords: SbH, transition properties, radiative lifetimes

PACS: 31.15.A–, 31.15.aj, 33.70.Ca **DOI:** 10.1088/1674-1056/ac6ee1

1. Introduction

The significance of the relativistic effect on the accurate descriptions of the transition properties of atoms and molecules containing heavy elements is well known in the quantum chemistry field.[1–3] With the increase in atomic number, the relativistic effects increase gradually. One example is the electronic triple-single transition that is forbidden by the electric dipole selection rule but becomes allowed in the heavy counterpart because of the spin–orbit coupling.

The spin-forbidden transitions in the low-lying states of group V hydrides have attracted considerable research interest because of the $\cdots(\pi^*)^2$ electron configuration. With regard to the antimony hydride molecule (SbH) as an example, early experiments were mainly focused on the spin-allowed transition $A^3\Pi \leftarrow X^3\Sigma^-$, and obtained accurate spectroscopic information of the ground state $X^3\Sigma^-$ via analysis of the absorption spectrum,[4] rotation spectrum,[5,6] and infrared spectrum.[7–9] Limited by the technology, the spin-forbidden transitions $b^1\Sigma^+/a^1\Delta$–$X^3\Sigma^-$ were not investigated until 1996. The vibration–rotation spectrum of the a2–$X_2 1$ and $b^1\Sigma^+_{0+}$–$X^3\Sigma^-_x$ of the SbH molecule were observed with a high-resolution Fourier transform spectrometer[9,10] and the spectroscopic constants of the $X^3\Sigma^-$, $a^1\Delta$, and $b^1\Sigma^+$ states were determined. Shestakov *et al.*[11] measured the $b^1\Sigma^+$–$X^3\Sigma^-$ transition of SbH using a laser-induced fluorescence spectrum, and obtained the radiative lifetime ($\tau = 173 \pm 3$ μs), the electric dipole transition moment ($\mu_0 = \pm 0.014$ ea_0 and $\mu_1 = \mp 0.023$ ea_0) and the magnetic dipole transition moments ($|M| = 1.62$ Bohr magnetons) of this transition. On the theoretical side, most of the research has focused on valence and Rydberg states. It is worth noting that Alekseyev *et al.*[12] utilized the MRD-CI method to calculate the transitions of SbH and obtained the electric transition dipole moments of the $b0^+$–$X_1 0^+$ and $b0^+$–$X_2 1$ transitions (0.00409 ea_0 and -0.02682 ea_0) and the radiative lifetime of the $b^1\Sigma^+$ ($v' = 0$) state (104 μs). The computed μ_1 agrees well with the experimental value, while the μ_0 value and the radiative lifetime deviate greatly from the experimental values.

Very recently, our group studied the electronic structure of the low-lying states of the SbH molecule, including spectroscopic and transition properties, with state of the art *ab initio* calculations using the internally contracted multireference configuration interaction method plus the Davidson correction (icMRCI + Q).[13] It showed that the radiative lifetime of the $b^1\Sigma^+$ state should be between 55 μs and 153 μs. There, we took account of spin–orbit coupling via the so-called state-interacting method. With the inclusion of several high-lying spin-free states, the calculated result is 153 μs; this is in reasonable agreement with the experimental value of 173 ± 3 μs,[11] while the deviation from the experiment still

†Corresponding author. E-mail: yanbing@jlu.edu.cn

© 2022 Chinese Physical Society and IOP Publishing Ltd

exists.

In most of the non-relativistic calculations on light atoms or molecules,[14–18] the use of the state-interacting method to account for spin–orbit coupling works quite well. It is nevertheless quite difficult dealing with the elements at the bottom of the periodic table because of the nature of perturbation theory, which is sensitive with regard to the number of spin-free (non-perturbated) states that participate in the computation. On the other hand, it is well known that the most straightforward method to consider the relativistic effect is to directly solve the 4-component Dirac equations. To double check our previous results and provide a benchmark for the spin-forbidden transitions $b^1\Sigma^+$–$X^3\Sigma^-$ of SbH theoretically, here, we reconsider the radiative lifetimes of the $b^1\Sigma^+$ state using the non-perturbated approach to deal with the relativistic effect, including both scalar correction and spin–orbit coupling, based on the exact 2-component (X2C) equation that can be derived from 4-component Dirac equations.

This paper is organized as follows. The computational method is described in Section 2. In Section 3 we present the computational results and discussions on the electronic transitions of SbH. Finally, a summary is presented in Section 4.

2. Computational details

In the present work, we performed the MRCI calculations based on the X2C Hamiltonians[19–23] for the electronic states of the SbH molecule with the DIRAC2019 code.[24,25]

For the Sb atom, we employed uncontracted core-valence Dyall basis sets: double-ζ (dyall.acv2z), triple-ζ (dyall.acv3z), and quadruple-ζ (dyall.acv4z).[26,27] For the hydrogen, we used Dyall's triple-ζ (dyall.v3z) and quadruple-ζ (dyall.v4z) basis sets.[28] The first set of calculations was carried out using the two-component Hartree–Fock method. Subsequently, the MRCI calculations, which are implemented in the KRCI module of DIRAC,[29–32] were performed.

Details of the settings of the generalized active spaces (GAS) used are listed in Table 1. The Sb $5\sigma_{1/2}$, $\sigma_{1/2}$, $\pi_{1/2}$, and $\pi_{3/2}$ and the antibonding $\sigma^*_{1/2}$ were placed in a complete active space (GAS II), yielding a distribution of six electrons in five Kramers pairs (6 in 5). Core–valence and core–core correlations were included by allowing up to two holes in the 4d shell (GAS I) of Sb. Finally, the electronic dynamic correlation is considered by the singles and doubles excitations from the combined spaces of GAS I and GAS II into the virtual spinor space (GAS III) corresponding to the energy thresholds of $1E_h$ and $5E_h$ (Hartree), respectively. We keep the remaining 36 electrons frozen; this means that we cause them to be occupied during the CI procedure.

The expressions of the complete basis set (CBS) limit are presented below:[33–37]

$$E_{\rm cbs} = E_n - A{\rm e}^{-(n-1)} - B{\rm e}^{-(n-1)^2}, \quad (n = 2,3,4), \tag{1}$$

$$E_n = E_{\rm cbs} + \frac{A}{n^3}, \quad (n = 3,4). \tag{2}$$

According to the potential energy curves (PECs) of the Ω states, the corresponding spectroscopic constants of the bound states were determined by resolving the one-dimensional nuclear Schrödinger equation with the aid of the LEVEL program,[38] including the excitation energy T_e, the equilibrium internuclear distance R_e, vibrational constants ω_e and the rotation constant B_e. The electric transition dipole moments (TDMs) were computed. Finally, the spontaneous radiative lifetimes of the several lowest energy transitions could be predicted.

Table 1. Generalized active spaces and occupation constraints for the SbH molecule in the symmetry double group $C_{\infty v}$.

GAS	Accumulation electron occupation		Kramers pairs	Function types
	Min.	Max.		
I	8	10	5	$\sigma_{1/2}$, $\pi_{1/2}$, $\pi_{3/2}$, $\delta_{3/2}$, $\delta_{5/2}$
II	14	16	5	$5\sigma_{1/2}$, $\sigma_{1/2}$, $\pi_{1/2}$, $\pi_{3/2}$, $\sigma^*{}_{1/2}$
III	16	16	$m^{a,b}$	virtual orbital

[a]Triple-ζ basis set: $m = 30$ ($1E_h$ threshold) and 50 ($5E_h$ threshold). [b]Quadruple-ζ basis set: $m = 50$ ($1E_h$ threshold) and 110 ($5E_h$ threshold).

3. Results and discussion

3.1. Spectroscopic constants of Ω states

We calculated the single-point energies of the lowest four states ($X^3\Sigma^+_{0+}$ [$X_1 0^+$], $X^3\Sigma^+_{0+}$ [$X_2 1$], $a^1\Delta_2$ [a2], and $b^1\Sigma^+_{0+}$ [$b0^+$]) in the Franck–Condon region using the MRCI method; the corresponding PECs are depicted in Fig. 1, and the data are listed in the supplementary material (Table I). These Ω states are deep well-bound states. From the computed energies of the Ω states, the corresponding spectroscopic constants of the bound states were determined. These results are tabulated in Table 2 together with available experimental and theoretical values for comparison.

It indicates that the spectroscopic constants tend to be more accurate with the increase in the cutoff energy and the improvement of the basis set. Taking Dyall's quadruple-ζ basis set and the cutoff energy 5 a.u. as an example, the R_e values

for the $X_1 0^+$ and $X_2 1$ states are calculated to be 1.6947 Å and 1.6937 Å, which are 0.0053 Å and 0.0082 Å smaller than the experimental values,[10,39] respectively. After considering the basis set extrapolations, the R_e value of the $X_1 0^+$ state can be close to 1.701 Å. The spin-splitting energy of the $X^3\Sigma^-$ state is 623.1 cm^{-1}, which is only 37 cm^{-1} underestimated from the experimental value of 660 cm^{-1}.[5] The spectroscopic constants of the $X_1 0^+$ and $X_2 1$ states are much closer to the experimental values than those calculated using our previous method.[13] The calculated values of R_e for the a2 and $b0^+$ states are 0.02407 Å (1.4%) and 0.02045 Å (1.2%) smaller than the experimental values,[10,11] and the errors of the corresponding T_e calculated value are 782.6 cm^{-1} (11.4%) and 625.2 cm^{-1} (4.6%), respectively.

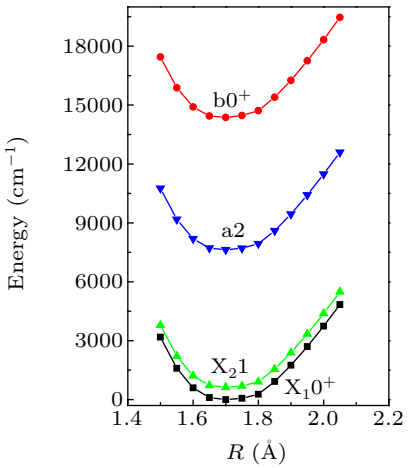


Fig. 1. The PECs for the $X_1 0^+$, $X_2 1$, a2, and $b0^+$ states with the Dyall's quadruple-ζ basis set and the cutoff energy 5 a.u.

Table 2. Computed spectroscopic constants of the Ω states for the $X_1 0^+$, $X_2 1$, a2, and $b0^+$ states.

Ω state	T_e (cm^{-1})	R_e (Å)	ω_e (cm^{-1})	B_e (cm^{-1})	Methods and references
$X_1 0^+$	0	1.7315	1920.6	5.5998	X2C Dyall's 3-ζ/1E_h threshold
	0	1.7343	1968	5.6053	X2C Dyall's 4-ζ/1E_h threshold
	0	1.6834	2303.7	5.9213	X2C Dyall's 3-ζ/5E_h threshold
	0	1.6947	1930.5	5.7826	X2C Dyall's 4-ζ /5E_h threshold
	0	1.7093	1929.6	5.6494	icMRCI + Q AWCVQZ-DK/AVQZ-DK[13]
	0	1.7077	1930.5	5.6629	icMRCI + Q AWCVQZ-PP/AVQZ[13]
	0	1.70		5.87	Expt.[39]
	0	1.722		5.684	Expt.[40]
	0	1.731	1886		MRD-CI[12]
	0	1.81	1763		RCI[41]
$X_2 1$	612	1.7313	1921.7	5.6024	X2C Dyall's 3-ζ/1E_h threshold
	558.4	1.7340	1970	5.6086	X2C Dyall's 4-ζ/1E_h threshold
	602	1.6829	2310.6	5.9262	X2C Dyall's 3-ζ/5E_h threshold
	623.1	1.6937	1938.2	5.7860	X2C Dyall's 4-ζ/5E_h threshold
	761.86	1.7092	1924.4	5.6717	icMRCI + Q AWCVQZ-DK/AVQZ-D[13]
	579.4	1.7076	1927.2	5.6836	icMRCI + Q AWCVQZ-PP/AVQZ[13]
		1.70187		5.86795	Expt.[10]
	660	1.729		5.684	Expt.[5]
	541	1.73	1892		MRD-CI[12]
	696	1.81	1762		RCI[41]
a2	8131.9	1.7266	1971.9	5.6648	X2C Dyall's 3-ζ/1E_h threshold
	7441.2	1.7309	1998.6	5.6476	X2C Dyall's 4-ζ/1E_h threshold
	7827.5	1.6810	2338.8	5.9436	X2C Dyall's 3-ζ/5E_h threshold
	7624.7	1.6904	1967.0	5.7979	X2C Dyall's 4-ζ /5E_h threshold
	7205.3	1.7068	1940.47	5.6848	icMRCI + Q AWCVQZ-DK/AVQZ-DK[13]
	7077.5	1.7051	1942.14	5.6957	icMRCI + Q AWCVQZ-PP/AVQZ[13]
	6842.1	1.71447	1942	5.78207	Expt.[10]
	7378	1.725	1904		MRD-CI[12]
	9362	1.81	1784		RCI[41]
$b0^+$	14740.3	1.7242	1993.8	5.6869	X2C Dyall's 3-ζ/1E_h threshold
	14265.4	1.7295	2003.4	5.6582	X2C Dyall's 4-ζ/1E_h threshold
	14596.5	1.6782	2376.7	5.9653	X2C Dyall's 3-ζ/5E_h threshold
	14365.6	1.6863	2001.9	5.8130	X2C Dyall's 4-ζ /5E_h threshold
	14225	1.7054	1946.39	5.6967	icMRCI + Q AWCVQZ-DK/AVQZ-DK[13]
	13921	1.7046	1940.63	5.8087	icMRCI + Q AWCVQZ-PP/AVQZ[13]
	13740.4	1.70675	1949.84	5.7900	Expt.[11]
	14129	1.721	1937		MRD-CI[12]
	15772	1.80	2061		RCI[41]

3.2. Analysis of the transition properties

Based on the above statements, we calculated the electric transition dipole moments of the $b0^+$–$X_1 0^+$ and $b0^+$–$X_2 1$ transitions and the results are depicted in Fig. 2. The data presented in this paper are included in the supplementary material (Tables II and III). As illustrated in Fig. 2, we found that the trends for two transitions are nearly linear with the changes in the internuclear distance.

For the $b0^+$–$X_1 0^+$ transition, the change of transition dipole moments obtained by the state interaction methods (a)–(d) is relatively slow with the increase in the internuclear distance, while those calculated using the relativistic methods (e)–(f) increase relatively rapidly. And from the curves from the relativistic method, the TDM values of the $b0^+$–$X_1 0^+$ transition are sensitive and improved with the increase in the basis set under the same cutoff energy of 1 a.u. (lines e and f in the upper panel of Fig. 2), while they are insensitive and with small improvement for the $b0^+$–$X_2 1$ transition; also, when the value reaches 5 a.u., the cutoff threshold greatly reduces the uncertainty of the basis sets. The above results indicate the stability and convergence of the present computational scheme. Thus, the basis set extrapolation and the effect of the cutoff threshold are necessary for consideration.

Table 3. The energy difference (cm^{-1}) and transition dipole moments (a.u.) of the $b0^+$–$X_1 0^+$ (μ_0) and $b0^+$–$X_2 1$ (μ_1) transitions at R_e and the radiative lifetime τ (μs) of the $b^1\Sigma^+$ ($v'=0$) for the different methods.

Method	$b0^+$–$X_1 0^+$ (μ_0)		$b0^+$–$X_2 1$ (μ_1)		$\tau(b^1\Sigma^+)$
	ΔE	TDM	ΔE	TDM	
Dyall's 3-ζ/1E_h threshold	14740	0.0116	14128	−0.027	199
Dyall's 4-ζ/1E_h threshold	14265	0.0137	13707	−0.0269	206
Dyall's 2-ζ/5E_h threshold	15091	0.0105	14507	−0.0314	146
Dyall's 3-ζ/5E_h threshold	14596	0.0113	13994	−0.0331	145
Dyall's 4-ζ/5E_h threshold	14367	0.0117	13744	−0.0336	148
CBS(2,3,4)[a]	14258	0.0144	13617	−0.0309	164
CBS(3,4)[a]	14228	0.0145	13585	−0.0310	163
Best estimated values	14243 ± 61	0.01445 ± 0.0002	13601 ± 73	−0.031 ± 0.0005	163.5 ± 7.5[b]
icMRCI + Q[13]	14224	0.0068	13463	−0.0356	153
MRD-CI[12]		0.0041		−0.0379	104
Expt.[11]		0.014		−0.0325	173 ± 3

[a]Extrapolation is performed with an energy threshold of 5 a.u. [b]See the text for error estimation.

The TDM values of the $b0^+$–$X_1 0^+$ and $b0^+$–$X_2 1$ transitions at R_e and the corresponding radiative lifetimes for the $b^1\Sigma^+$ ($v'=0$) state are listed in Table 3. According to Table 3, the values of μ_0 reported using our previous calculations[13] and other theoretical calculations[12] are about a factor of two to three lower than the experimental value, while their μ_1 values agree well with the experimental value.[11] At R_e, the transition dipole moments of the $b0^+$–$X_2 1$ (μ_1) transition with a cutoff energy of 5 a.u. are −0.0331 a.u. and −0.0336 a.u., respectively, with different basis sets; the best estimated value averaged with formulas (1) and (2) is -0.031 ± 0.005, which is only about 0.001 a.u. overestimated when compared with the experimental value (−0.0325 a.u.). For the $b0^+$–$X_1 0^+$ transition, the best estimated value of μ_0 is in excellent agreement with the experimental value,[11] and all experimental significant digits are reproduced. The total radiative lifetime τ of the $b^1\Sigma^+$–$X^3\Sigma^-$ transition is obtained according to the following formula:

$$1/\tau = 1/\tau_1 + 1/\tau_2, \tag{3}$$

where τ_1 and τ_2 represent the radiative lifetimes of the $b0^+$–$X_1 0^+$ and $b0^+$–$X_2 1$ branch transitions, respectively, and τ represents the radiative lifetimes of the $b^1\Sigma^+$–$X^3\Sigma^-$ transition; that is, the spontaneous radiative lifetimes of the $b^1\Sigma^+$ state.

Considering the incompleteness of the basis sets, the two-parameter and three-parameter basis set extrapolation formulas are used to extrapolate the energies and TDM, and obtain the radiative lifetime range (163.5 ± 0.5 μs). The two extrapolation schemes (formulas (1) and (2)) determine the uncertainty arising from the basis sets. The detailed data are presented in Table 3. Next, we proceed with uncertainty analysis, and here we mainly consider the influence of the truncated threshold on the energy difference (ΔE) and TDM. For the $b0^+$–$X_1 0^+$ transition, the uncertainties of ΔE and TDM are 46 cm^{-1} and 0.0001 a.u. while, for the $b0^+$–$X_2 1$ transition, the uncertainties are 57 cm^{-1} and 0.0005 a.u., respectively. Due to the propagation of the uncertainty of the energy difference and TDM, we determined that the error bars of the radiative lifetime for the $b^1\Sigma^+$ ($v'=0$) state are 7 μs. Taking the averaged values of the two extrapolation results as the reference value, the combinations of this value and the uncertainties caused by the extrapolation and truncation threshold are selected as 'best estimated values'. Among these values, the best radiative life-

time of the $b^1\Sigma^+$ $(\upsilon' = 0)$ state is 163.5 ± 7.5 μs, which is in reasonable agreement with the experimental value (173 ± 3 μs) measured by Shestakov *et al.*[11] The present work improves 10 μs ($\sim 7\%$) and 60 μs ($\sim 60\%$) values of the total lifetime of the $b^1\Sigma^+$ $(\upsilon' = 0)$ state compared with our previous and other theoretical computations and, more importantly, predicts reasonable electric dipole moment values of branch transitions.

Table 4. The transition dipole moments (a.u.) and the radiative lifetime τ (s) of the $X_1 0^+$–$X_2 1$ and $X_2 1$–a2 transitions at R_e.

Method	$X_1 0^+$–$X_2 1$		$X_2 1$–a2	
	TDM (a.u.)	τ	TDM (a.u.)	τ
X2C Dyall's 3-ζ/5E_h threshold	0.00638	58.2	0.0131	7.6 (−3)
X2C Dyall's 4-ζ/5E_h threshold	0.00660	48.6	0.0132	8.2 (−3)
MRD-CI[12]		105	0.00829	23 (−3)

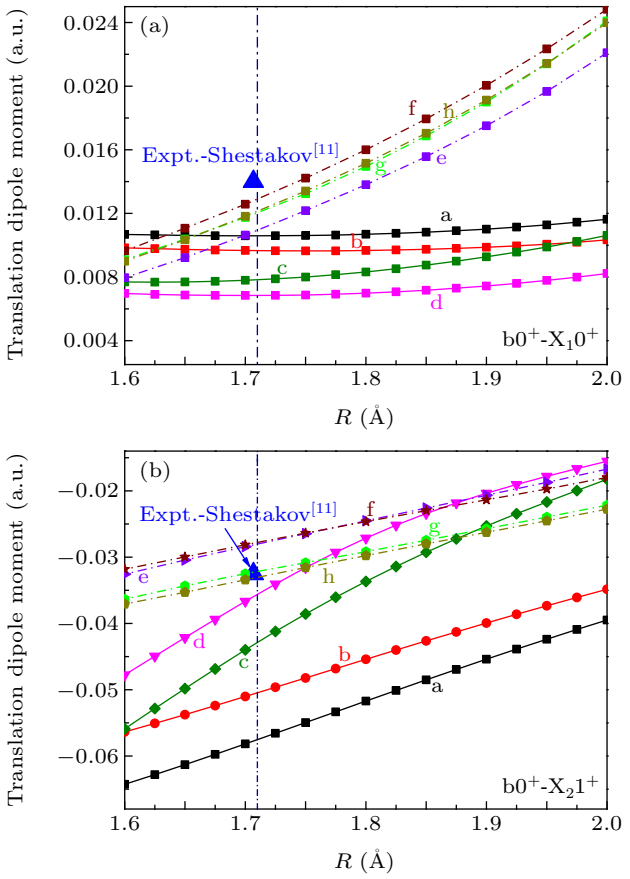


Fig. 2. The transition dipole moments of the $b0^+$–$X_1 0^+$ and $b0^+$–$X_2 1$ transitions for SbH. (a) The results of all-electron basis set calculations for the state interaction technique; (b) the results of pseudopotential basis set calculations for the state interaction technique; (c) the same as (a), but with high-lying states included; (d) the same as (b), but with high-lying states included; (e) the results of Dyall's 3-ζ basis set and energy threshold of 1 Hartree for the relativistic method; (f) the results of Dyall's 4-ζ basis set and energy threshold of 1 Hartree for the relativistic method; (g) the same as (e), but the energy threshold is 5 Hartree; (h) the same as (f), but the energy threshold is 5 Hartree.

Based on the reasonable results of the $b0^+$–$X_1 0^+$ and $b0^+$–$X_2 1$ transitions using the (g)–(h) computational schemes, we also analyzed the transition dipole moments and the corresponding radiative lifetimes of the $X_1 0^+$–$X_2 1$ and $X_2 1$–a2 transitions. The results are shown in Fig. 3 and Table 4, and detailed data of the transition dipole moments are included in the supplementary material (Table IV and Table V). As shown in Fig. 3, the transition strength decreases with the increase in the bond distance. At R_e, the transition dipole moments of the $X_1 0^+$–$X_2 1$ transition are 0.00638 a.u. and 0.00660 a.u. under the Dyall's triple-ζ and quadruple-ζ basis sets, and the corresponding spontaneous radiative lifetimes of the $X_2 1$ $(\upsilon' = 0)$ state are obtained as 58.2 s and 48.6 s, respectively. These two values are about half of the theoretical result of 105 s obtained by Alekseyev.[12] However, since the radiative lifetime of the $b^1\Sigma^+$ state obtained by this group has a difference of about 40% from the experimental value,[11] our results have certain credibility based on this analysis. Furthermore, the spontaneous radiative lifetimes for the a2 $(\upsilon' = 0)$ state are calculated to be ~ 8 ms.

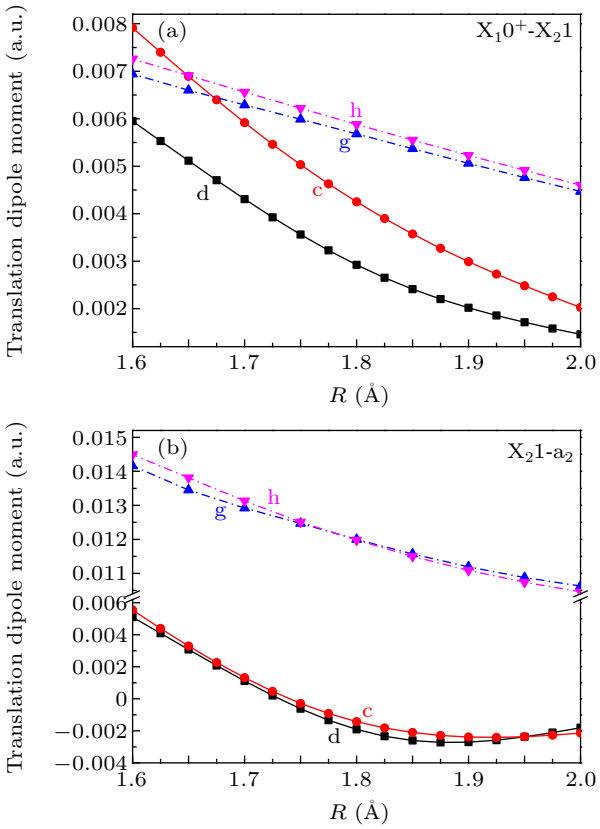


Fig. 3. The transition dipole moments of the $X_1 0^+$–$X_2 1$ and $X_2 1$–a2 transitions for SbH. The meanings of the symbols c, d, g, and h in the figure are the same as those of the remarks in Fig. 2.

4. Conclusion

Calculations on the transition properties of the first three states of the SbH molecule were performed under the relativistic framework with the aid of the exact two-component Hamiltonians (X2C). The spectroscopic constants for the first four Ω excited states were determined and compared with the previous values. In terms of transitions, the radiative lifetimes of the $b^1\Sigma^+$ $(\upsilon' = 0)$ state were calculated. The best result of

163.5 ± 7.5 μs is in reasonable agreement with the experimental value (173 ± 3 μs). The spontaneous radiative lifetimes of the $X_2 1$ ($v' = 0$) and a2 ($v' = 0$) states are calculated to be 48.6 s and ~ 8 ms, respectively. The present work predicts not only the value of the total lifetime of the $b^1\Sigma^+$ ($v' = 0$) state but also the reasonable electric dipole moment values of branch transitions. The present work is a benchmark computation of the electric dipole moments and lifetime of transitions in the SbH molecule, and is of great theoretical significance for the selection of computational schemes in further transition properties investigations in heavy elements containing molecular systems.

Data availability statement

The data that support the findings of this study are openly available in Science Data Bank at https://www.doi.org/10.11922/sciencedb.j00113.00018.

Acknowledgments

We are grateful for the computational support from the High Performance Computing Center (HPCC) of Jilin University and the high performance computing cluster Tiger@IAMP. Project supported by the National Natural Science Foundation of China (Grant No. 11874177).

References

[1] Schwerdtfeger P 2004 *Relativistic Electronic Structure Theory Part 2. Applications* (Amsterdam: Elsevier) pp. 2-6
[2] Hess B A 2003 *Relativistic Effects in Heavy-Element Chemistry and Physics* (Chichester: Wiley) pp. 71–73
[3] Tian H C, Xu L Q and Zhu L F 2018 *Chin. Phys. B* **27** 043101
[4] Basco N and Yee K K 1968 *Spectrosc. Lett.* **1** 13
[5] Bollmark P and Lindgren B 1974 *Phys. Scr.* **10** 325
[6] Bollmark P, Lindgren B and Sassenberg U 1981 *Phys. Scr.* **24** 542
[7] Urban R D, Essig K and Jones H 1993 *J. Chem. Phys.* **99** 1591
[8] Wang X, Souter P F and Andrews L 2003 *J. Phys. Chem. A* **107** 4244
[9] Yu S, Fu D, Shayesteh A, Gordon I E, Appadoo D R T and Bernath P 2005 *J. Mol. Spectrosc.* **229** 257
[10] Beutel M, Setzer K D, Shestakov O and Fink E H 1996 *J. Mol. Spectrosc.* **179** 79
[11] Shestakov O, Gielen R, Pravilov A M, Setzer K D and Fink E H 1998 *J. Mol. Spectrosc.* **191** 199
[12] Alekseyev A B, Liebermann H P, Lingott R M, Bludsky O and Buenker R J 1998 *J. Chem. Phys.* **108** 7695
[13] Liu Y, Ren X Y, Xiao Z Y and Yan B 2021 *J. Quant. Spectrosc. Radiat. Transfer* **258** 107394
[14] Zhang X M, Yan P Y, Li R, Gai Z Q, Liang G Y, Xu H F and Yan B 2016 *J. Quant. Spectrosc. Radiat. Transfer* **180** 154
[15] Xiao Z Y, Ren X Y, Liu Y and Yan B 2021 *J. Quant. Spectrosc. Radiat. Transfer* **267** 107624
[16] Feng S, Shan S M, Guo H J, Xu H F and Yan B 2019 *J. Phys. Chem. A* **123** 3435
[17] Xue J L, Yuan X, Li R, Liu X S, Xu H F and Yan B 2020 *Spectroc. Acta Pt. A-Molec. Biomolec. Spectr.* **241** 118679
[18] Ren X Y, Xiao Z Y, Liu Y and Yan B 2021 *Chin. Phys. B* **30** 053101
[19] Liu W and Peng D 2009 *J. Chem. Phys.* **131** 031104
[20] Kutzelnigg W and Liu W 2005 *J. Chem. Phys.* **123** 241102
[21] Liu W and Peng D 2006 *J. Chem. Phys.* **125** 044102
[22] Peng D, Liu W, Xiao Y and Cheng L 2007 *J. Chem. Phys.* **127** 104106
[23] Cheng L 2019 *J. Chem. Phys.* **151** 104103
[24] Saue T, Bast R, Gomes A S P, Jensen H J A, Visscher L, Aucar I A, Remigio R D, Dyall K G, Eliav E, Faßhauer E, Fleig T, Halbert L, Hedegård E D, Helmich-Paris B, Iliaš M, Jacob C R, Knecht S, Laerdahl J K, Vidal M L, Nayak M K, Olejniczak M, Olsen J M H, Pernpointner M, Senjean B, Shee A, Sunaga A and Stralen J N P 2020 *J. Chem. Phys.* **152** 204104
[25] Gomes A S P, Saue T, Visscher L, *et al.* 2019 *DIRAC, a relativistic ab initio electronic structure program*, Release DIRAC19
[26] Dyall K G 2002 *Theor. Chem. Acc.* **108** 335
[27] Dyall K G 2006 *Theor. Chem. Acc.* **115** 441
[28] Dyall K G 2016 *Theor. Chem. Acc.* **135** 128
[29] Fleig T, Olsen J and Visscher L 2003 *J. Chem. Phys.* **119** 2963
[30] Fleig T, Jensen H, Olsen J and Visscher L 2006 *J. Chem. Phys.* **124** 104106
[31] Visscher L 2002 *J. Compt. Chem.* **23** 759
[32] Knecht S, Jensen H J Aa and Fleig T 2010 *J. Chem. Phys.* **132** 014108
[33] Peterson K A, Woon D E and Dunning T H 1994 *J. Chem. Phys.* **100** 7410
[34] Peterson K A, Lyons J R and Francisco J S 2006 *J. Chem. Phys.* **125** 084314
[35] Deng D, Lian Y and Zou W 2017 *Chem. Phys. Lett.* **688** 33
[36] Vasilyev V 2017 *Comput. Theor. Chem.* **1115** 1
[37] Yang X, Xu H F and Yan B 2019 *Chin. Phys. B* **28** 013203
[38] Le Roy R J 2017 *J. Quant. Spectrosc. Radiat. Transfer* **186** 167
[39] Bollmark P and Lindgren B 1967 *Chem. Phys. Lett.* **1** 480
[40] Huber K P and Herzberg G 1979 *Molecular Spectra and Molecular Structure* (New York: Van Nostrand Reinhold Company) p. 572
[41] Balasubramanian K, Tanpipat N and Bloor J E 1987 *J. Mol. Spectrosc.* **124** 458